EUROPEAN ORGANIZATION FOR NUCLEAR RESEARCH

L3 Note 2574
June 30, 2000

Improved Studies with Longitudinally and Transversely Polarised $W^{\pm}$ Bosons

The L3 Collaboration

Abstract

Preliminary results of the $W^{\pm}$ bosons helicity fractions, using the 1997, 1998 and 1999 data taking period at center–of–mass energies between 183–202 GeV, are presented. Combining the new data with the published data at center–of–mass energies of 183 GeV and 189 GeV the fractions of the different W helicity states, −1, +1 and 0 are measured to be 56.2±4.5%, 17.9±2.3% and 25.9±3.5% respectively. The results agree well with the SM expectation for the three W helicity states of 57.6%, 17.6% and 24.8%, averaging the different center–of–mass energies. The data sample is then used to: (1) measure the helicity fractions for W^+ and W^- decays separately. The measured helicity fractions agree within the statistical errors and provide the first direct test of CP invariance in the reaction $e^+e^- \rightarrow W^+W^-$; (2) demonstrate the variation of the W helicity fractions with the W polar scattering angle; (3) to provide evidence for WW spin correlations.

Submitted to the *XXXth International Conference on High Energy Physics*
July 27 - August 2, 2000, Osaka, Japan

1 Overview

The analysis and results presented in this note include the 1997, 1998 and 1999 data samples, which essentially doubles the statistics compared to that used for the L3 publication on the "Direct Observation of Longitudinally Polarised W bosons" [1].

The main objectives of this note are (1) to repeat and update the measurements of the W helicity fractions at slightly higher center–of–mass energies and (2) to improve the statistical significance especially of the W polarisation results as a function of the W scattering angle with respect to the beam direction. Furthermore, the enlarged data sample is used to test the CP invariance in the reaction $e^+e^- \rightarrow W^+W^-$ by comparing the W^+ and W^- helicity fractions separately and finally to provide evidence for WW spin correlations.

The event selection criteria for the 1999 data and the analysis method are identical to the ones described in [1]. For details about the analysis and references we refer to this publication.

2 Inclusive W polarisation measurements

In the 1999 data sample, 673 events with an estimated background of 4%, independent of the center–of–mass energies are selected as candidates for the reaction $e^+e^- \rightarrow W^+W^- \rightarrow \ell\nu q\bar{q}$. Splitting the 1999 (1997+1998) data sample into $W \rightarrow e\nu$ and $W \rightarrow \mu\nu$ candidates, 350 (369) with electrons and 323 (329) with muons events are selected. Separating the 1999 data into the $\sqrt{s} = 192$ GeV, 196 GeV, 200 GeV and 202 GeV center–of–mass samples, 102, 243, 212 and 116 WW candidate events are selected respectively. Various other distributions do not show significant variations between the 1999 data and the published 1997 and 1998 data samples. Because of the preliminary nature of the systematic error study, a systematic error of ±3%, twice as large as the one determined for the 1998 data sample, is assigned for the measurement of the W helicity fractions.

Table 1 gives the results for the inclusive W helicity fractions as measured with leptonic and hadronic W decays for the 4 different center–of–mass energies in the 1999 data and the KORALW Monte Carlo. For completeness the published results for the 1997 and 1998 data samples are repeated. The W helicity fractions are in agreement and do not indicate any systematic trend and the statistical errors for the measured W helicity fractions are large compared to expected variations of the W helicity at the different center–of–mass energies.

The fit results, allowing for transverse and longitudinal W helicity states for the 1999 data period and for the 1997–1999 data period are shown in Figure 1 and 2 respectively. The hadronic and leptonic W decays are only described if all three W helicity states are used to fit the data. Combining the results for the leptonic and hadronic W decays the measured helicity fractions for the 1999 data and the combined 1997–1999 data are given in Table 2. Combining all data, the fractions of the different W helicity states, –1, +1 and 0 are measured to be 56.2±4.5%, 17.9±2.3% and 25.9±3.5% respectively and agree well with the SM expectation of 57.6%, 17.6% and 24.8%.

2.1 Test of the CP invariance

Within the Standard Model, CP is conserved in the reaction $e^+e^- \rightarrow W^+W^-$ and the helicity fractions (+1, –1 and 0) for the W^+ are expected to be identical with (–1, +1 and 0) for the W^- respectively. One can thus test the CP invariance by measuring separately the helicity fractions for W^+ and W^-.

For this measurement, the charge of the W bosons is obtained from the leptonic $W^{\pm} \to \ell^{\pm}\nu$ decay, while the opposite charge is associated to the hadronically decaying W. Using this assignment, 682 $W^{+} \to \ell^{+}\nu$ and 689 $W^{-} \to \ell^{-}\bar{\nu}$ are identified in the entire data sample. After correcting for background and efficiency the W helicity fractions are obtained from the fits for the leptonic and hadronic W decays as shown in Figure 3. Within the errors the helicity fractions for W^{+} and W^{-} agree for both W decay modes. The results, combining both W decay modes are given in Table 2 and agree with the assumption of CP invariance.

2.2 Measurement of the W helicity fractions as a function of the W scattering angle

The inclusive W helicity fractions are also studied as a function of the W^{-} polar scattering angle $\Theta_{W^{-}}$ with respect to the e^{-} beam direction using four different bins in $\cos\Theta_{W^{-}}$. The corresponding data and fit results for the W helicity fractions with the leptonic W decays are shown in Figure 4. Strong variations of the W helicity compositions are clearly seen. The quantitative results are given in Table 3 and Figure 5 and are in agreement with the Standard Model expectations.

3 Study of WW spin correlations

In contrast to spin correlations studies with photon pairs, spin correlations of massive vector bosons have not been observed so far. Spin correlations between the W^{+} and W^{-} produced in the reaction $e^{+}e^{-} \to W^{+}W^{-}$ would mean that the helicity fractions measured with the leptonically decaying W bosons depend on the helicity of the hadronically decaying W.

One can thus use the above method to measure the W helicity fractions of leptonically decaying W as a function of the decay angle, $|\cos\theta^{*}_{thrust}|$ of the hadronically decaying W. Without the knowledge of the quark charge one can only enrich or deplete the fractions of hadronically decaying W with helicity ± 1.

Another possible manifestation of WW spin correlations would show that the relative orientation of the two W decay planes shows a correlation.

The goal of the measurements described below is thus to find evidence for spin correlations of pair produced W^{+} and W^{-}.

3.1 WW spin correlations with respect to the W flight direction

Within the Standard Model and at center–of–mass energies close to 190 GeV one expects that about 45% of the $W^{-}W^{+}$ events are produced in the helicity combination (–1, +1) and about 10% with the helicity combination (0, 0). In addition, one expects substantial contributions from WW helicity combinations: (+1, –1); (0, –1) or (+1, 0); (–1, 0) or(0, +1) and (+1, +1) or (–1, –1). The relative contributions for these helicity combinations are expected to depend strongly on the W^{-} polar scattering angle, $\Theta_{W^{-}}$, with respect to the e^{-} beam direction. For example, the fraction of $W^{-}W^{+}$ events with helicity (–1, +1) is largest for $0.3 < \cos\Theta_{W^{-}} < 0.9$. Consequently, not only the inclusive fraction of W^{-} (W^{+}) bosons with helicity -1 ($+1$) increases but in particular the fraction of $W^{-}W^{+}$ pairs where the W^{-} boson is found with helicity -1 and the W^{+} with $+1$.

To study WW spin correlations we analyse the distribution of the charged lepton decay angle, $\cos\theta^{*}_{lepton}$, as a function of the corresponding decay angle $|\cos\theta^{*}_{thrust}|$ of the hadronically decaying W. Within the limited statistics three subsamples for $|\cos\theta^*_{thrust}|$, 0–0.33, 0.33–0.66 and 0.66–1.0 are used. This separation results in a depletion ($0 < |\cos\theta^*_{thrust}| < 0.33$) or an enrichment ($0.66 < |\cos\theta^*_{thrust}| < 1.0$) of hadronically decaying $\mathrm{W} \rightarrow q\bar{q}$ bosons with helicity ± 1.

In addition, to enhance possible effects the event sample is further divided into three intervals for the W^- scattering angle, $\cos\Theta_{\mathrm{W}^-}$, with respect to the beam direction. The intervals $-0.9 < \cos\Theta_{\mathrm{W}^-} < -0.3$, $-0.3 < \cos\Theta_{\mathrm{W}^-} < 0.3$ and $0.3 < \cos\Theta_{\mathrm{W}^-} < 0.9$ are used. Within the Standard Model one expects large variations of the different WW helicity combinations for these bins.

After correcting for background and efficiency, the measured leptonic decay angle distributions, $\cos\theta^*_{lepton}$, in the data and the KORALW Monte Carlo are analysed.

The normalized distributions for leptonic W decays in data and the KORALW Monte Carlo are shown in Figures 6–8 for the subsamples where the hadronic W decays are found in the depleted or enriched ± 1 helicities configuration. The resulting helicity fractions for the various subsamples in the data and the KORALW Monte Carlo are summarized in Table 4. The obtained numbers show some variations for the selected subsamples of hadronically decaying W boson decays and are thus indications for WW spin correlations.

The strongest variation of the lepton decay angle distribution is seen for $0.3 < \cos\Theta_{\mathrm{W}^-} < 0.9$ as shown in Figure 8. This correlation is slightly stronger than in the KORALW Monte Carlo as can be seen from the quantitative results in Table 4.

We have studied a variety of possible systematics, including the event selection criteria, the hadron energy response function, the dependence on the center–of–mass energy and uncertainties from the efficiency and bias corrections. All these studies are limited by the data statistics but no significant systematic effect has been found and adding all uncertainites the systematic uncertainties are found to be always smaller than half of the statistical errors.

3.2 WW spin correlations with respect to the W decay planes

Finally the difference between the decay angles, $\Delta\phi^*$, reconstructed from the two W decay planes is analysed. The $\Delta\phi^*$ distribution, shown in Figure 9, is found to be in good agreement with the expectations from the KORALW Monte Carlo where a slight preference for large angles between the decay planes is expected. Quantitatively, the distribution can be fitted with the function $1 + D \times \cos(2 \times |\Delta\phi^*|)$ [2]. The resulting value for D is found to be -0.061 ± 0.040 in the data which differs by 1.5 standard deviations from uncorrelated decay planes ($D = 0$) and agrees well with the expectation from the KORALW Monte Carlo with $D = -0.061 \pm 0.006$.

4 Summary

The inclusive W helicity fractions and WW spin correlations have been measured using the reaction $\mathrm{e^+e^-} \rightarrow \mathrm{W^+W^-} \rightarrow \ell\nu\mathrm{q\bar{q}}$ with 1371 candidate events at center–of–mass energies between 183 GeV and 202 GeV.

The measured inclusive W helicity fractions are in excellent agreement with the Standard Model and demonstrate the expected variation as a function of the W^- scattering angle with the e^- beam direction. Furthermore, the helicity fractions of W^+ and W^- are in good agreement with the expectations from the CP invariance in the production of WW pairs.

The data indicate the existence of WW boson spin correlations, with a significance of more than three standard deviations along the W flight direction. The observed WW correlations are slightly stronger than the ones expected from the Monte Carlo simulation.

In addition, the decay planes of the two W bosons appear to be correlated with a significance of about 1.5 standard deviations. This correlation agrees with the one simulated in the KORALW Monte Carlo.

References

[1] M. Acciarri *et al.*, Phys. Lett. **B474** (2000) 194–204.

[2] M. J. Duncan and G. L. Kane and Wayne W. Repko, Phys. Rev. Lett. **55** (1985) 773.

	Helicity W $\rightarrow \ell\nu$			Helicity W$\rightarrow$ hadrons	
$\sqrt{s} = 202$ GeV					
	-1	$+1$	0	±1	0
Data	0.635 ± 0.18	0.185 ± 0.11	0.18 ± 0.22	1.0 ± 0.21	0.0 ± 0.20
MC	0.61	0.16	0.23	0.77	0.23
$\sqrt{s} = 200$ GeV					
	-1	$+1$	0	±1	0
Data	0.65 ± 0.12	0.23 ± 0.07	0.12 ± 0.12	0.40 ± 0.13	0.60 ± 0.14
MC	0.61	0.17	0.22	0.78	0.22
$\sqrt{s} = 196$ GeV					
	-1	$+1$	0	±1	0
Data	0.49 ± 0.11	0.12 ± 0.06	0.39 ± 0.12	0.69 ± 0.14	0.31 ± 0.13
MC	0.60	0.17	0.23	0.77	0.23
$\sqrt{s} = 192$ GeV					
	-1	$+1$	0	±1	0
Data	0.62 ± 0.18	0.32 ± 0.11	0.05 ± 0.20	0.65 ± 0.20	0.35 ± 0.20
MC	0.57	0.18	0.25	0.75	0.25
$\sqrt{s} = 189$ GeV					
	-1	$+1$	0	±1	0
Data	0.568 ± 0.071	0.212 ± 0.046	0.220 ± 0.077	0.716 ± 0.086	0.285 ± 0.084
MC	0.56	0.18	0.26	0.74	0.26
$\sqrt{s} = 183$ GeV					
	-1	$+1$	0	±1	0
Data	0.56 ± 0.14	0.10 ± 0.08	0.34 ± 0.15	0.75 ± 0.17	0.25 ± 0.17
MC	0.53	0.20	0.27	0.73	0.27

Table 1: Measured W helicity fractions for the leptonic and hadronic W decays for the different center–of–mass energies for the 1999 data taking period and the corresponding Standard Model expectations as implemented in the KORALW Monte Carlo program. For completeness, the published results for the $\sqrt{s} = 189$ GeV and $\sqrt{s} = 183$ GeV data samples are also given.

$\sqrt{s} = 192 - 202$ GeV			
W helicity	-1	$+1$	0
Data	0.541 ± 0.063	0.174 ± 0.032	0.285 ± 0.053
MC	0.60	0.17	0.23
$\sqrt{s} = 183 - 202$ GeV			
Data	0.562 ± 0.045	0.179 ± 0.023	0.259 ± 0.035
MC	0.576	0.176	0.248
W^- helicity	-1	$+1$	0
Data(W^-)	0.565 ± 0.060	0.181 ± 0.032	0.254 ± 0.049
W^+ helicity	$+1$	-1	0
Data(W^+)	0.559 ± 0.068	0.177 ± 0.036	0.264 ± 0.049

Table 2: Measured W helicity fractions, combining the leptonic and hadronic W decays for the 1999 data ($\sqrt{s} = 192 - 202$ GeV) and the 1997–1999 data ($\sqrt{s} = 183 - 202$ GeV samples). The corresponding helicity fractions in the Standard Model, luminosity averaged, are also given. The helicity fractions, separated for W^- and W^+ are given in the lower part.

$\sqrt{s} = 183 - 202$ GeV Data			
$\cos\Theta_{W^-}$	-1	$+1$	0
$-1.0 - -0.4$	0.185 ± 0.08	0.345 ± 0.11	0.47 ± 0.10
$-0.4 - \ \ 0.3$	0.475 ± 0.07	0.27 ± 0.05	0.25 ± 0.07
$0.3 - \ \ 0.9$	0.685 ± 0.07	0.15 ± 0.03	0.17 ± 0.05
$0.9 - \ \ 1.0$	0.55 ± 0.14	0.0 ± 0.05	0.45 ± 0.10
$\sqrt{s} = 183 - 202$ GeV KORALW MC			
$\cos\Theta_{W^-}$	-1	$+1$	0
$-1.0 - -0.4$	0.126	0.448	0.426
$-0.4 - \ \ 0.3$	0.424	0.290	0.286
$0.3 - \ \ 0.9$	0.713	0.122	0.165
$0.9 - \ \ 1.0$	0.639	0.028	0.335

Table 3: The W helicity fractions measured as a function of $\cos\Theta_{W^-}$ combining hadronic and leptonic W decays and for $\sqrt{s} = 183 - 202$ GeV in data and Monte Carlo.

$\sqrt{s} = 183 - 202$ GeV Data				
		$W \to \ell\nu$		
$\cos\Theta_{W^-}$	$W \to q\bar{q}$	-1	$+1$	0
$-0.9 - -0.3$	±1 depleted	0.240 ± 0.10	0.349 ± 0.14	0.411 ± 0.20
$-0.9 - -0.3$	±1 enriched	0.060 ± 0.06	0.252 ± 0.16	0.688 ± 0.19
$-0.9 - -0.3$	difference	0.18 ± 0.011	0.097 ± 0.21	-0.277 ± 0.28
$-0.3 - 0.3$	±1 depleted	0.549 ± 0.13	0.451 ± 0.11	0.0 ± 0.18
$-0.3 - 0.3$	±1 enriched	0.505 ± 0.13	0.202 ± 0.09	0.293 ± 0.15
$-0.3 - 0.3$	difference	0.044 ± 0.19	0.249 ± 0.14	-0.293 ± 0.24
$0.3 - 0.9$	±1 depleted	0.262 ± 0.13	0.169 ± 0.09	0.570 ± 0.16
$0.3 - 0.9$	±1 enriched	0.862 ± 0.13	0.127 ± 0.05	0.011 ± 0.086
$0.3 - 0.9$	difference	-0.600 ± 0.018	0.042 ± 0.10	0.559 ± 0.18
$\sqrt{s} = 183 - 202$ GeV KORALW MC				
		$W \to \ell\nu$		
$\cos\Theta_{W^-}$	$W \to q\bar{q}$	-1	$+1$	0
$-0.9 - -0.3$	±1 depleted	0.181	0.373	0.445
$-0.9 - -0.3$	±1 enriched	0.145	0.506	0.349
$-0.9 - -0.3$	difference	0.036	-0.133	0.096
$-0.3 - 0.3$	±1 depleted	0.461	0.253	0.286
$-0.3 - 0.3$	±1 enriched	0.426	0.305	0.269
$-0.3 - 0.3$	difference	0.035	-0.052	0.017
$0.3 - 0.9$	±1 depleted	0.648	0.149	0.203
$0.3 - 0.9$	±1 enriched	0.768	0.100	0.133
$0.3 - 0.9$	difference	-0.12	0.049	0.070

Table 4: The W helicity fractions measured with leptonic W decays for different intervals of $\cos\Theta_{W^-}$ and with the enriched and depleted subsamples of the hadronically decaying W bosons for $\sqrt{s} = 183 - 202$ GeV in data and Monte Carlo.

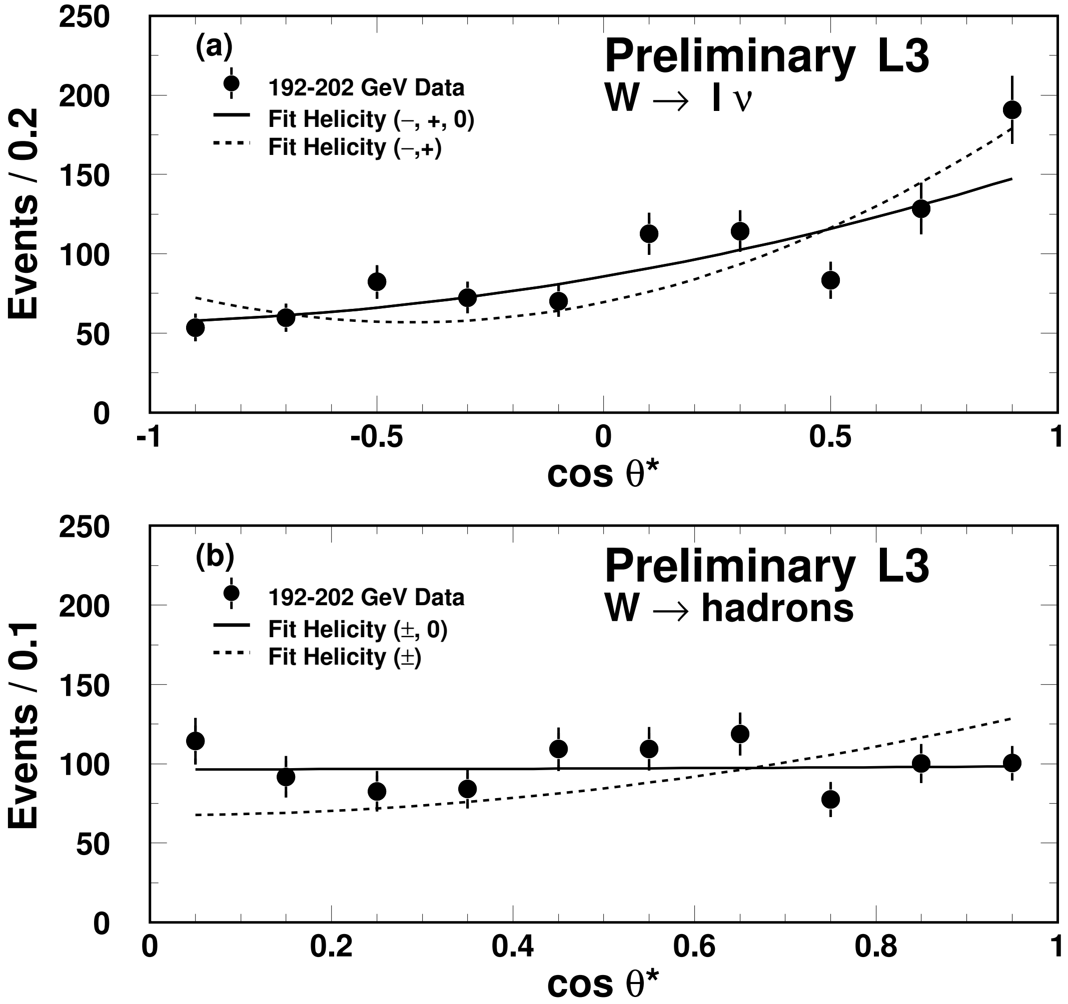

Figure 1: Corrected $\cos\theta^*$ distributions for (a) leptonic W decays and (b) for hadronic W decays at $\sqrt{s} = 192 - 202$ GeV. The fit results for the different W helicity hypotheses are also shown. For leptonic W decays the χ^2 increases from 19.2 for seven degrees of freedom if all three W helicity states are included to 32.0 for eight degrees of freedom if only helicity -1 and $+1$ are used to describe the data. For hadronic W decays the χ^2 increases from 11.3 for eight degrees of freedom if all three W helicity states are included to 38.3 for nine degrees of freedom if only helicity ±1 are used to describe the data.

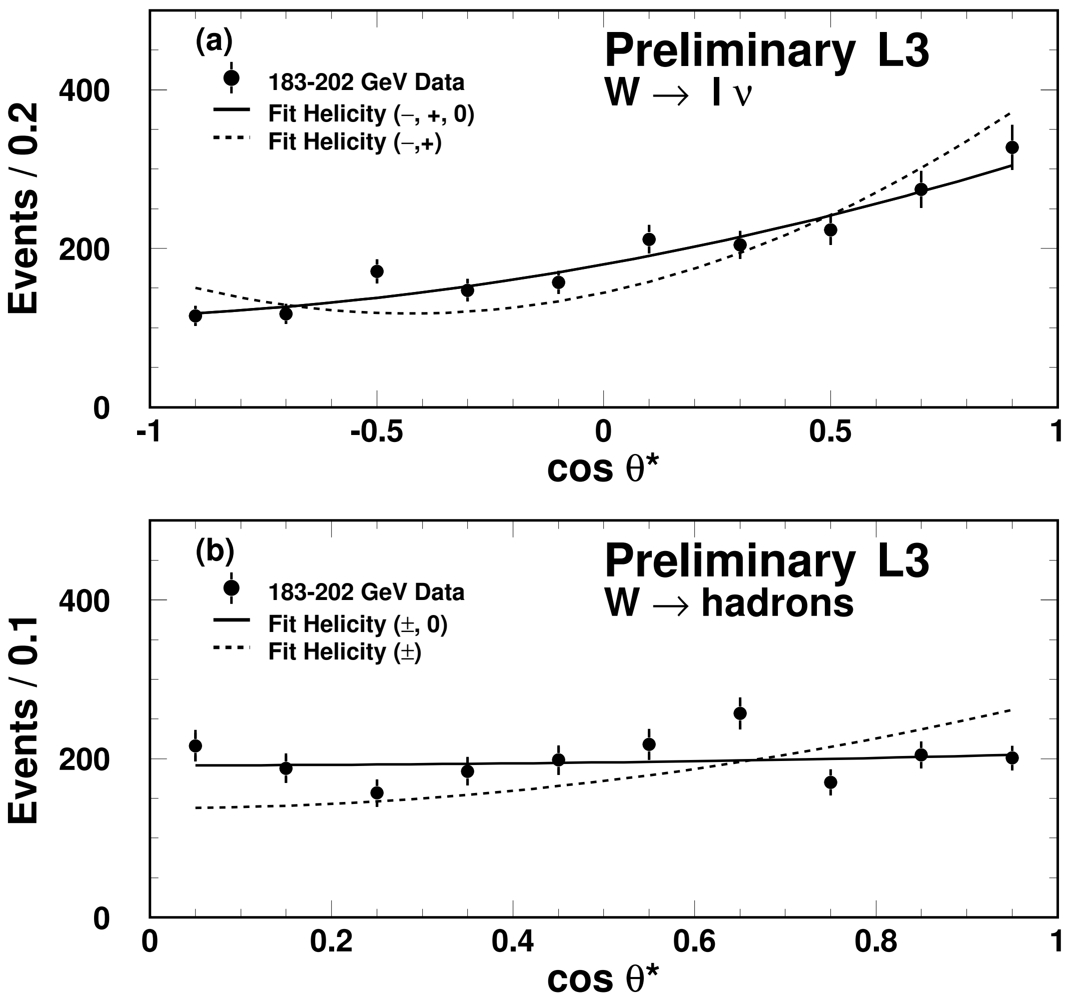

Figure 2: Same as Figure 1 but for combined sample with center–of–mass energies from $\sqrt{s} = 183 - 202$ GeV. For leptonic W decays the χ^2 increases from 9.5 for seven degrees of freedom if all three W helicity states are included to 40.8 for eight degrees of freedom if only helicity -1 and $+1$ are used to describe the data. For hadronic W decays the χ^2 increases from 19.4 for eight degrees of freedom if all three W helicity states are included to 68.1 for nine degrees of freedom if only helicity ±1 are used to describe the data.

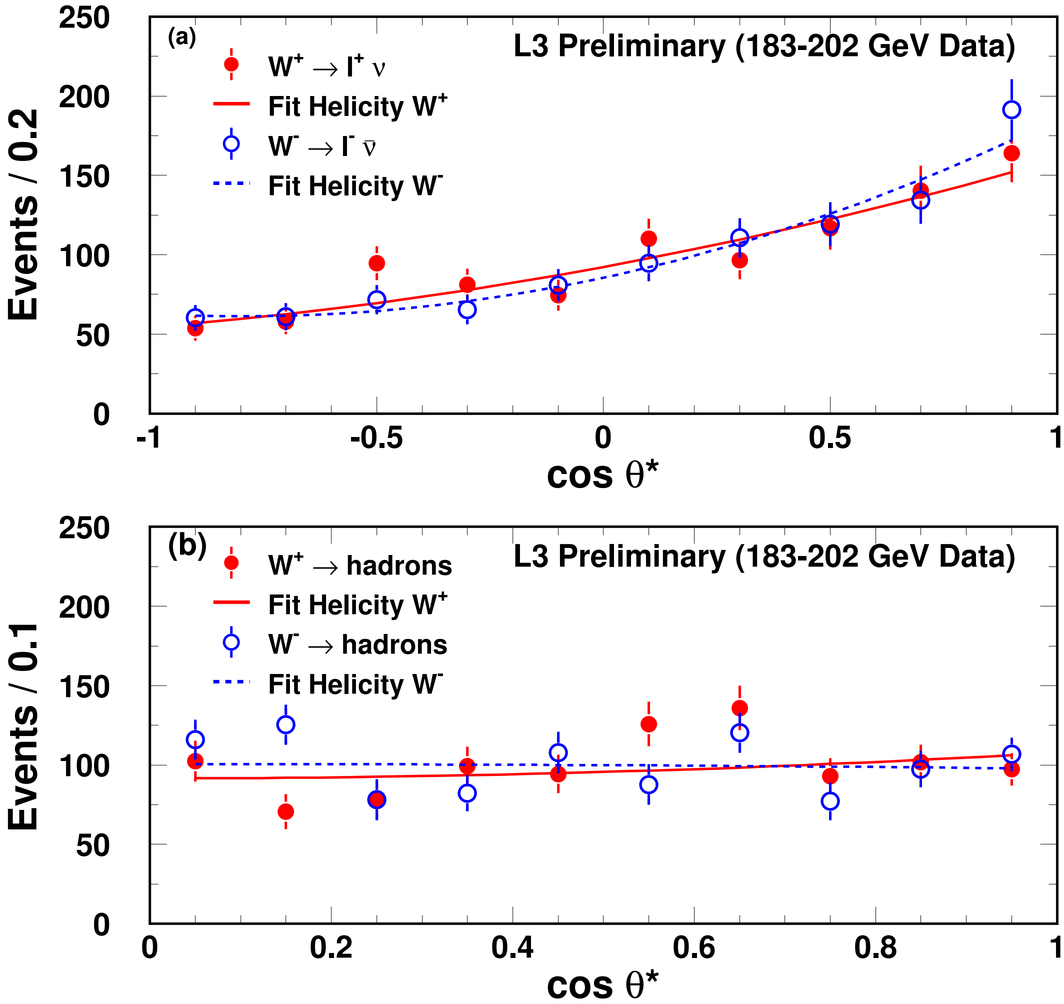

Figure 3: Corrected $\cos\theta^*$ distributions for (a) leptonic W decays and (b) for hadronic W decays at $\sqrt{s} = 183 - 202$ GeV separated for W^+ and W^- together with the corresponding fits for the different W helicities.

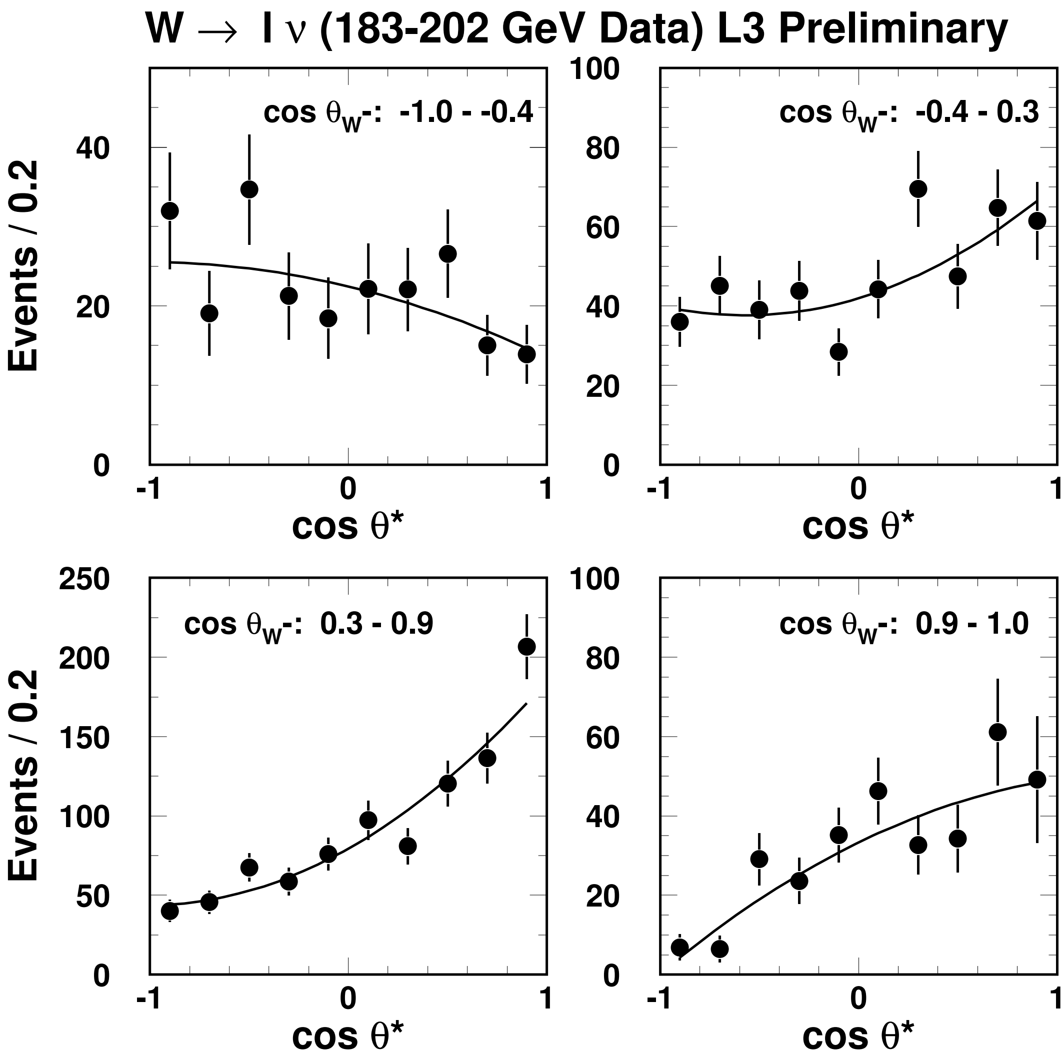

Figure 4: Corrected $\cos\theta^*$ distributions for leptonic W decays separated into 4 different W^- scattering angles with respect to the e^- beam direction and the entire data sample. The fit results for three different W helicity hypotheses are also shown.

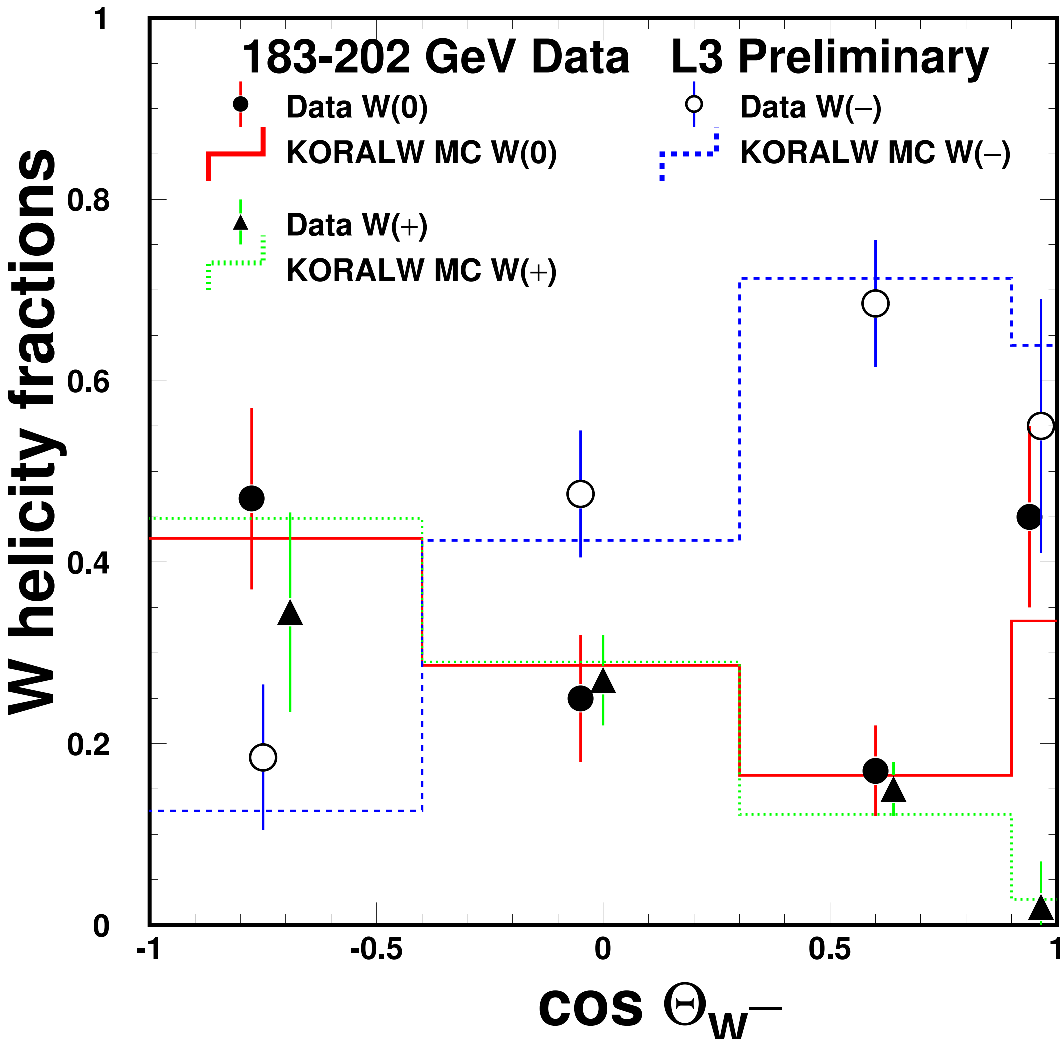

Figure 5: W helicity fractions f_0 and f_- for four different bins of $\cos\Theta_{W^-}$ in the combined data sample and in the KORALW Monte Carlo.

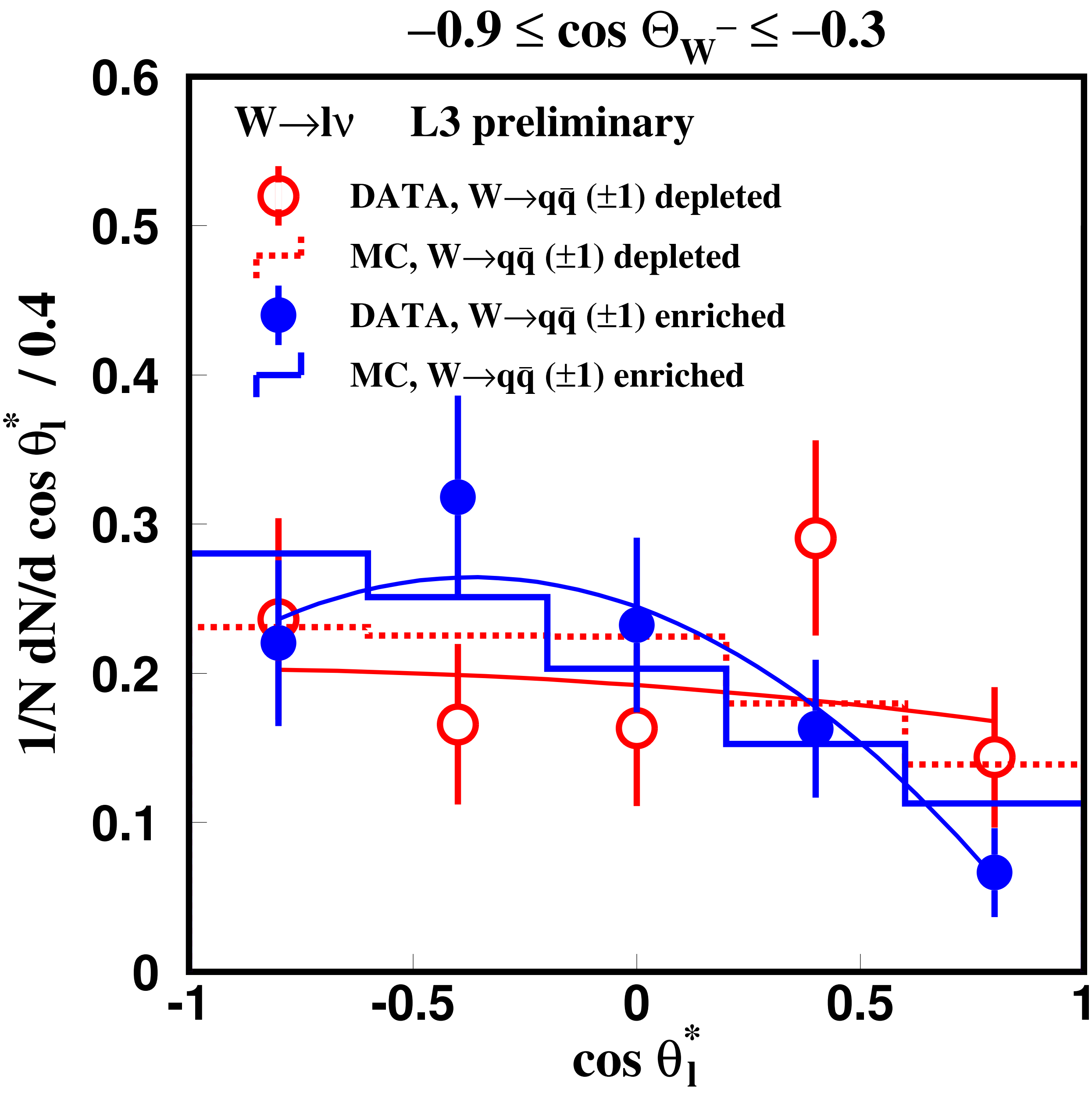

Figure 6: Corrected and normalized $\cos\theta_\ell^*$ distributions for $W \to \ell\nu$ decays for data and the KORALW Monte Carlo in the interval $-0.9 < \cos\Theta_{W^-} < -0.3$. The distributions are shown for the subsamples of hadronic W decays with ±1 helicities depleted or enriched.

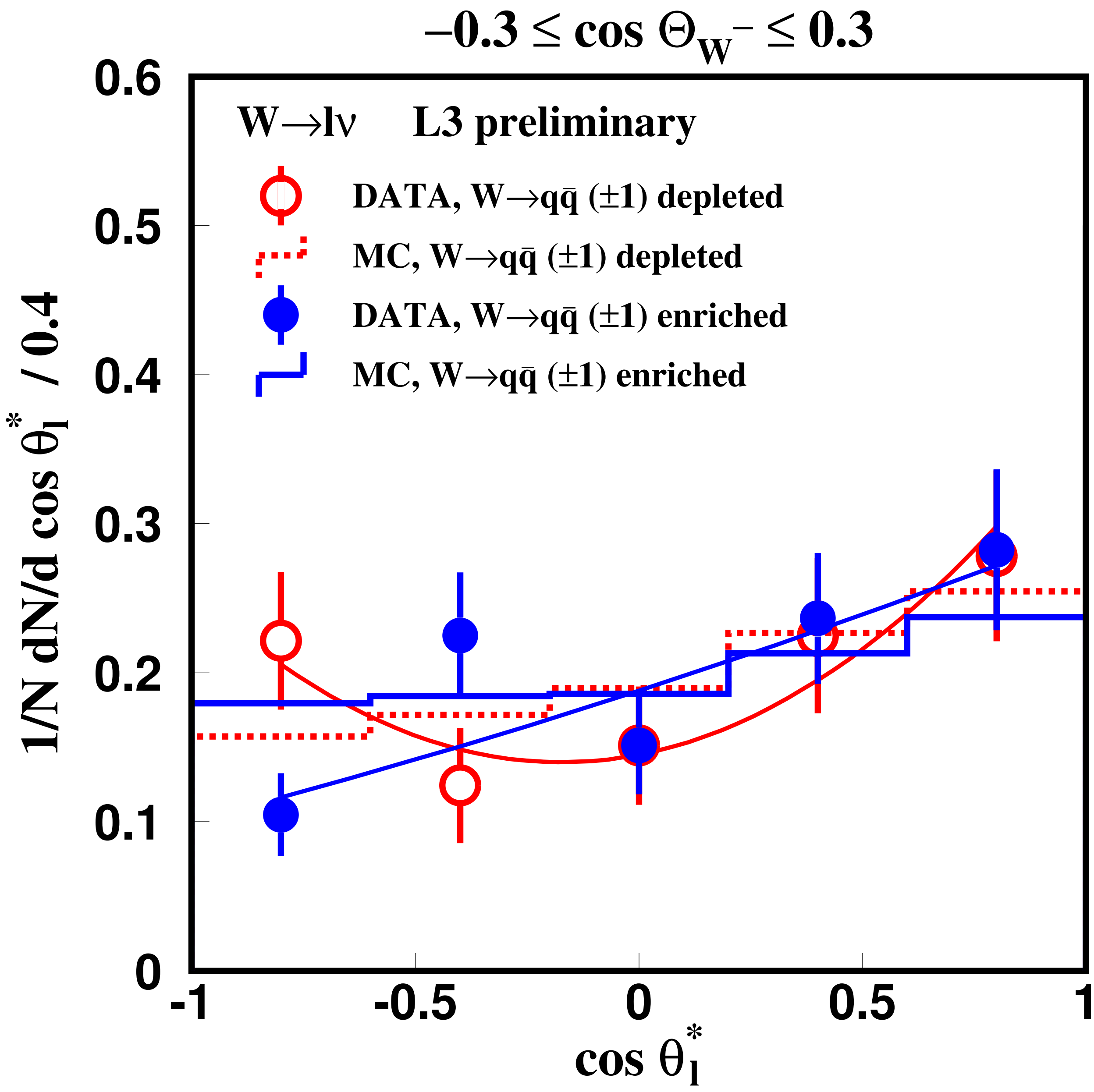

Figure 7: Corrected and normalized $\cos\theta_\ell^*$ distributions for $W \to \ell\nu$ decays for data and the KORALW Monte Carlo in the interval $-0.3 < \cos\Theta_{W^-} < 0.3$. The distributions are shown for the subsamples of hadronic W decays with ±1 helicities depleted or enriched.

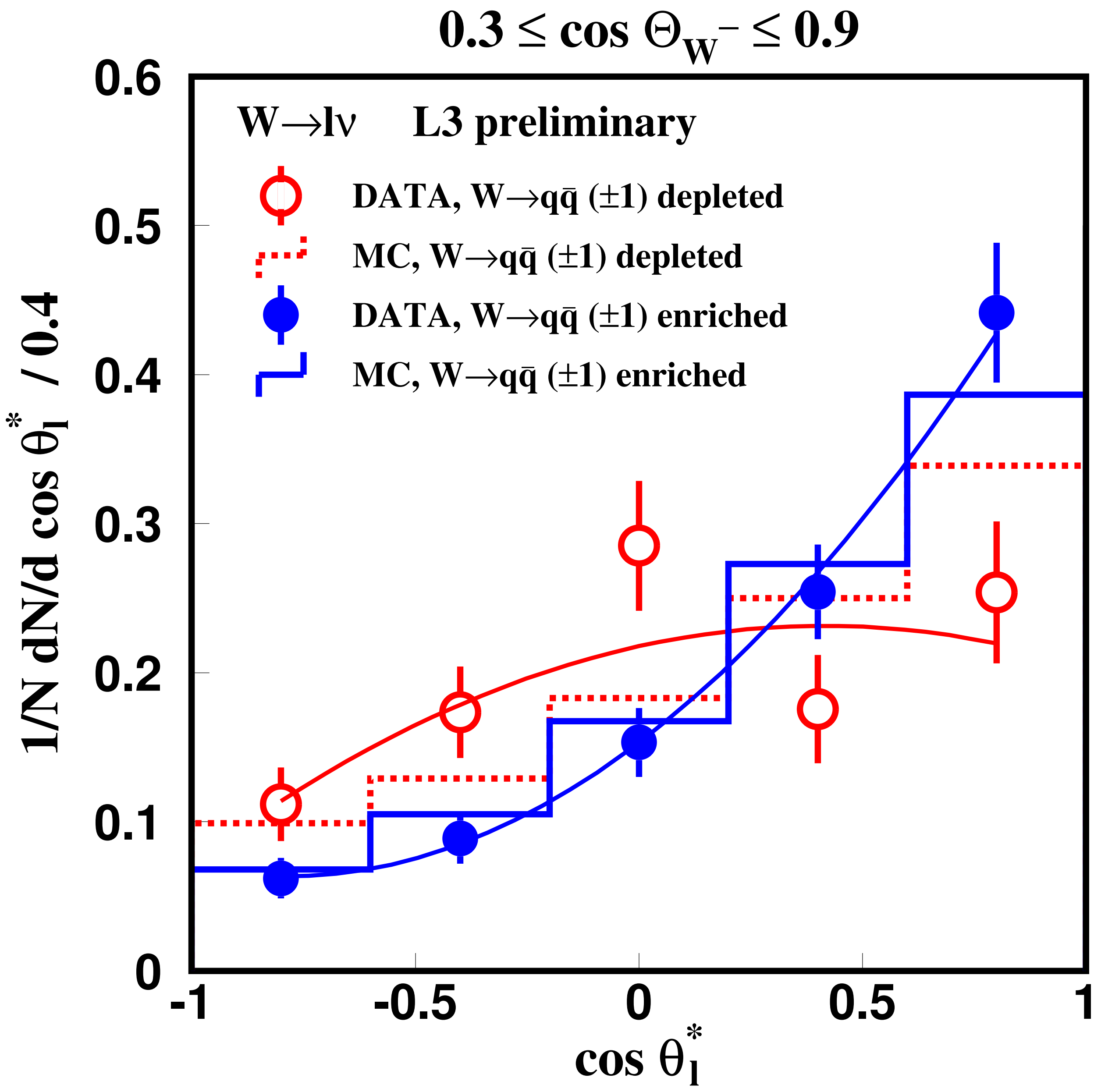

Figure 8: Corrected and normalized $\cos\theta^*_\ell$ distributions for $W \to \ell\nu$ decays for data and the KORALW Monte Carlo in the interval $0.3 < \cos\Theta_{W^-} < 0.9$. The distributions are shown for the subsamples of hadronic W decays with ±1 helicities depleted or enriched.

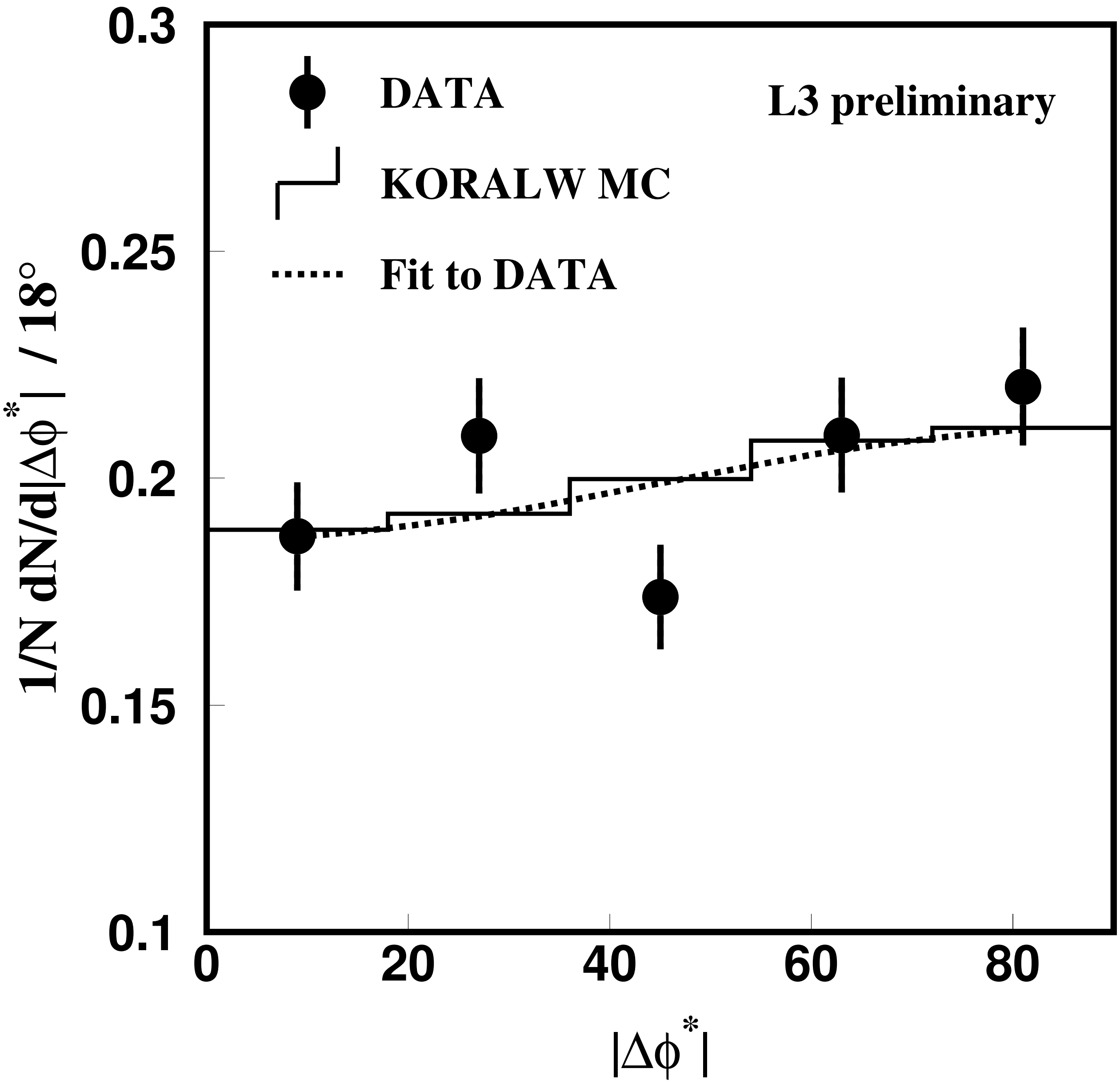

Figure 9: Distribution of the angle between the W^+W^- decay planes in the data and the KORALW Monte Carlo. Uncorrelated W decays would show a flat distribution.